NANO LETTERS

Letter

pubs.acs.org/NanoLett

Mechanical Stiffening of Porphyrin Nanorings through Supramolecular Columnar Stacking

Simon A. Svatek,[†] Luis M. A. Perdigão,[†] Andrew Stannard,[†] Maria B. Wieland,[†] Dmitry V. Kondratuk,[‡] Harry L. Anderson,[‡] James N. O'Shea,[†] and Peter H. Beton*[,†]

[†]School of Physics & Astronomy, University of Nottingham, Nottingham, NG7 2RD, United Kingdom

[‡]Department of Chemistry, University of Oxford, Chemistry Research Laboratory, Oxford, OX1 3TA, United Kingdom

Supporting Information

ABSTRACT: Solvent-induced aggregates of nanoring cyclic polymers may be transferred by electrospray deposition to a surface where they adsorb as three-dimensional columnar stacks. The observed stack height varies from single rings to four stacked rings with a layer spacing of 0.32 ± 0.04 nm as measured using scanning tunneling microscopy. The flexibility of the nanorings results in distortions from a circular shape, and we show, through a comparison with Monte Carlo simulations, that the bending stiffness increases linearly with the stack height. Our results show that noncovalent interactions may be used to control the shape and mechanical properties of artificial macromolecular aggregates offering a new route to solvent-induced control of two-dimensional supramolecular organization.

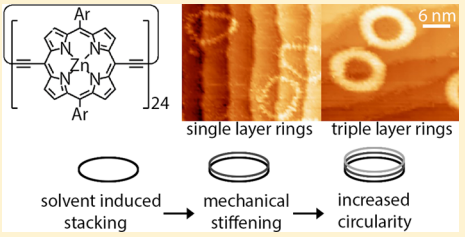

KEYWORDS: *STM, electrospray, porphyrin, polymer, π−π stacking, Monte Carlo*

The use of noncovalent interactions to control the relative placement of molecules on surfaces has been exploited for the formation of a wide variety of two-dimensional supramolecular networks with tailored dimensions, symmetry, and functionality.[1−3] The component molecules in these arrays are typically small and may be considered rigid, but there has recently been growing interest in the adsorption and on-surface synthesis of much larger and more flexible species, such as extended one-dimensional polymers and other molecules which exhibit conformational freedom.[4−11] The precise conformation of an adsorbed polymer is difficult to control since the intramolecular elastic energy associated with the intrinsic flexibility of the molecule can be comparable with intermolecular and molecule−surface interactions. We show here that noncovalent interactions may be used to control the shape of flexible polymers by exploiting a newly observed, and unexpected, supramolecular organization of cyclic porphyrin polymer nanorings into stacked columns. The nanorings are deposited using electrospray, and the stacking arises from a solvent-dependent aggregation which is preserved after deposition. The stacking results in an increase in the bending stiffness of the polymer nanorings and a transition to a near circular shape. Our results provide an analogue of the conformational control afforded by tertiary structure and self-assembly in biopolymers. We demonstrate that solvent-induced supramolecular organization can be used to control the shape of artificial macromolecular aggregates with molecular weights comparable with those of many naturally occurring proteins.

Porphyrin molecules attract widespread interest due to their optoelectronic properties and have been investigated widely across the physical[12] and biological[13] sciences. In recent work the synthesis of a new type of porphyrin-derived nanostructure, a cyclic polymer nanoring, has been demonstrated.[14,15] These butadiyne-linked nanorings are synthesized using a template-directed strategy, via the formation of Vernier self-assemblies. These new materials attract great interest[16−18] due to the delocalized nature of their molecular orbitals and their similarity to the biological light-harvesting complexes LH1 and LH2.[19,20] Using the Vernier-templating approach, it is possible to synthesize nanorings with precise control of the number of porphyrin groups, and it has been possible to isolate cyclic structures with 6, 8, 12, 16, 18, and 24 porphyrin units.[14,15] A schematic diagram of c-P24, the nanoring with 24 linked Zn porphyrins, is shown in Figure 1A. Octyloxy side chains are attached to the porphyrin macrocycle via aryl groups to promote solubility. The center-to-center porphyrin spacing in analogue linear polymers is 1.33 nm, implying a diameter of 10.16 nm (the separation of diametrically opposed Zn atoms) for c-P24 assuming a circular conformation.

We have investigated c-P24 and also c-P12, the analogue cyclic polymer with 12 porphyrin units, using scanning tunneling microscopy (STM) following deposition of the nanorings on an Au(111) surface using electrospray. This technique permits the direct transfer of large molecules, which are not compatible with sublimation, from solution into an ultrahigh vacuum system (base pressure 2×10^{-10} Torr).[21−23] For our experiments the solution concentration was 100 μg/mL of nanorings in a methanol/toluene mixture (1:3 by volume), or the same solution with added 5% by volume

Received: May 13, 2013
Revised: June 18, 2013
Published: June 21, 2013

   dx.doi.org/10.1021/nl4017557 | *Nano Lett.* 2013, 13, 3391−3395

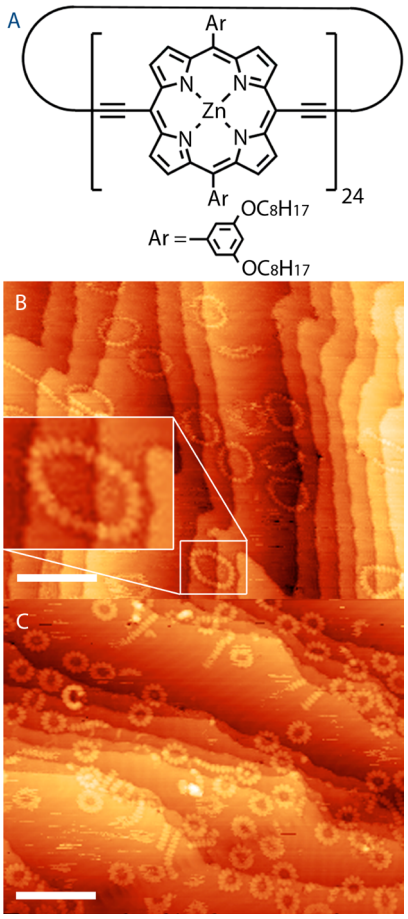

Figure 1. (A) Chemical structure of c-P24. (B) c-P24 on Au(111) deposited from methanol/toluene 1:3, 5% pyridine. (C) c-P12 on Au(111) deposited from methanol/toluene 1:3. Scanning parameters: tunnel current, 30 pA, sample voltage −1.8 V (B), −2.0 V (C). Scale bars: 20 nm (B, C).

tetrahydrofuran (THF) or pyridine. The solution was passed at a flow rate of ∼10 μL/min through a stainless steel emitter held at ∼1.8 kV under atmospheric conditions. A highly directional jet of droplets then enters the vacuum system via a narrow capillary tube, passes through a series of differentially pumped skimmer apertures, and then impinges on a gold substrate. Further experimental details are included in Supporting Information.

Figure 1B shows an STM image following the deposition of c-P24 from a solution with added pyridine. The 24 individual porphyrin units may be clearly resolved (see for example inset to Figure 1B), and in common with nearly all adsorbed c-P24 at low coverage, we find that adsorption occurs preferentially with the nanoring overlapping one or more step edges on the Au(111) surface (in many cases one or two porphyrin macrocycles partially overlap the step edge resulting in an appearance of the step running tangentially to the ring edge; further images for lower c-P24 coverage are included in the Supporting Information). The topographic height (typically 0.1 nm) and uniformity of contrast of the nanorings indicate that the porphyrin units are adsorbed parallel to the surface, although some distortion of the porphyrin macrocycle[24] cannot be ruled out from our images. The conformation for c-P24 shows a significant deviation from a circular shape; for example the nanoring in Figure 1B inset has long and short axes equal to 12 and 7 nm, respectively. This implied flexibility is consistent with our previous studies of analogue linear polymers with average lengths of ∼50 nm which exhibit bending with a radius of curvature as small as 1.3 nm, equivalent to a 180° degree turn over a circumference of ∼3 porphyrin repeat units.[5]

Figure 1C shows, for comparison, images of c-P12, an analogue nanoring with 12 porphyrin units which are also preferentially adsorbed at Au terrace steps. For c-P12 the deviation from a circular shape is much reduced as compared with c-P24. The observation of a preferential adsorption site indicates that both the c-P12 and c-P24 nanorings may diffuse intact across the surface following adsorption and that the barrier for diffusion, even for such mesoscale structures (c-P24 has dimensions ∼10 nm and a molecular weight of ∼25 kDa), may be overcome at room temperature on experimental time scales (for other examples of macromolecular adsorption and diffusion see Deng et al.[8] and Tanaka and Kawai[25]).

The rational formation of covalent links prior to deposition offers a novel and alternative route to the organization of porphyrins on surfaces and may be contrasted with the approach adopted in many previous studies where positional control of porphyrins is realized through the incorporation of side groups which promote supramolecular organization or covalent bond formation through Ullmann-type on-surface reactions.[26−28] In addition the observed stacking represents a new route to supramolecular organization perpendicular to a surface.[29]

The surface topography is significantly different if the c-P24 nanorings are deposited without the addition of pyridine to the toluene/methanol mixture (see Figure 2A). In this case we

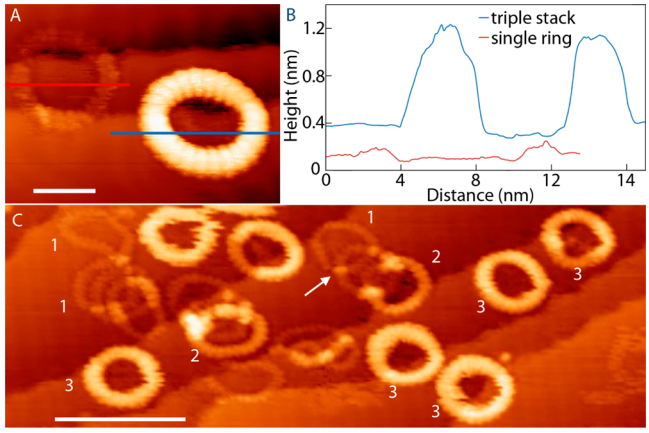

Figure 2. (A) STM image of a single height (left), and stacked (right) c-P24 nanoring deposited from methanol/toluene 1:3. Scale bar 6 nm. (B) Height profile of the blue and red marked traces shows the different ring heights. (C) Larger area shows different ring heights for triple (3), double (2), and single (1) rings. The arrow indicates the crossing point of overlapping nanorings. Scale bar 20 nm. Tunnel current, 30 pA, sample voltage −1.8 V.

observe nanorings which have different apparent heights, 0.1 and 0.8 nm, respectively, for the left and right nanoring in Figure 2A, although 24 porphyrin subunits may still be resolved. In larger area images (see Figure 2C) we observe nanorings with different heights and also many which are partially overlapping. Also observed in Figure 2C (top center) is a nanoring which appears less stable under these scanning conditions; this may be due to a less stable adsorption site remote from the step edges.

dx.doi.org/10.1021/nl4017557 | Nano Lett. 2013, 13, 3391−3395

A histogram (Figure 3A) shows that nanoring heights are clustered around discrete values, and we therefore ascribe the

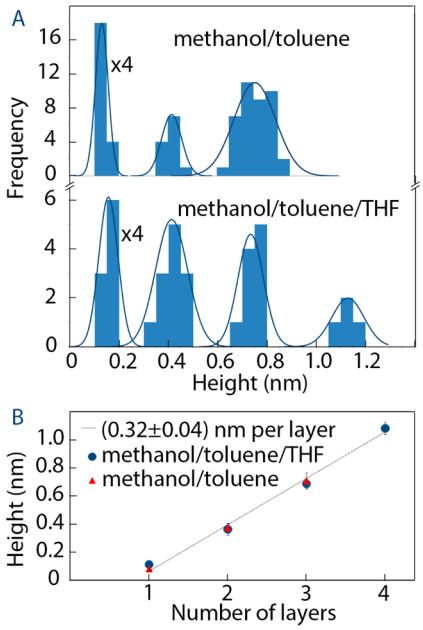

Figure 3. (A) Histogram of nanoring heights from different solutions (upper, methanol–toluene 1:3; lower, the same methanol–toluene mixture with 5% (by volume) THF added). The peaks for heights <0.2 nm have been scaled down for clarity. (B) Peak position in the histogram versus the peak number.

higher features to stacks of two and three nanorings. We have analyzed similar images acquired using a solution with added THF (5%), and the relevant histogram is also shown in Figure 3A. Heights are clustered at similar values, although we observe in this case a structure with apparent height of 1.1 nm, corresponding to four layers.

In Figure 3B the histogram peak position is plotted versus peak number and is found to be linear with a gradient, corresponding to the layer spacing in the stacks, of 0.32 ± 0.04 nm. This value is consistent with parallel alignment of porphyrin groups and stabilization of the stacked nanorings by $\pi-\pi$ interactions.[30,31]

Also present on the surface are partially overlapping nanorings (see Figure 2C). The height of the crossing points of two single layer rings corresponds to that of a double layer stacked ring (see arrow in Figure 2C; for height profiles and a discussion of the crossing of double and single layer rings see Supporting Information), providing further evidence that the high contrast nanorings arise from stacking.

The dependence on solvent indicates that the columnar stacks are preformed prior to deposition on the surface. The formation of such stacks through alternative mechanisms where rings are adsorbed as monomers and then undergo organizational changes leading to the observed structures are highly unlikely and would not be expected to have a dependence on solvent. Furthermore the stacked nanorings are, like the single layers, found to be preferentially adsorbed at step edges indicating that these complex aggregates can diffuse intact across the surface following adsorption.

The addition of pyridine to the solution of c-P24, which inhibits the nanoring stacking, also results in a color change from red to green. UV–visible–NIR titrations show that the Q-band shifts to shorter wavelengths (from 850 to 820 nm) and that the B-band becomes narrower (at around 480 nm) on addition of pyridine; both of these spectral changes indicate that pyridine causes dissociation of stacked aggregates.[32,33] It is well-known that amine ligands such as pyridine can prevent the aggregation of metalloporphyrins by axial coordination to the central metal cation, and these observations provide further support that the stacking occurs in solution prior to deposition.

The stacked nanorings in Figure 2 have a shape which is closer to circular than the single height rings. The deviation from circularity is characterized by the parameter $g = a/b - 1$, where a and b are, respectively, the long and short axes of a nanoring. For an ellipse g is related to the flattening factor, f ($g = fb/a$) and for a circle $g = 0$. We find a systematic dependence of g on stack height with a mean value, $\bar{g} = 0.55 \pm 0.05$ for a single layer, a lower value for a double layer, 0.31 ± 0.08, while for triple layers $\bar{g} = 0.28 \pm 0.03$. For comparison $\bar{g} = 0.27 \pm 0.02$ for single layers of c-P12.

The reduction in the value of g implies an increased mechanical stiffness of the nanoring as the number of stacked rings is increased. The deformation energy, E, due to bending of a continuous elastic ring is proportional to κ_B, the bending stiffness, and is given by a path integral of the local curvature $C(s)$, where s is the loop coordinate, around the ring,[34]

$$E = \frac{\kappa_B}{2} \oint C(s)^2 \mathrm{d}s \qquad (1)$$

For an ellipse the relationship between E and g may be determined analytically.[35] For the nanorings considered here, the shapes are less regular so a numerical approach is required. Accordingly we use Monte Carlo simulations to calculate $\bar{g}$ for a segmented elastic ring in thermal contact with a heat bath at temperature T and use these calculated values to estimate the variation of bending stiffness with stack height.

To model a c-PN nanoring, N bending points, labeled by index i, are defined at positions $\{r_i\}$ with an equilibrium separation L which is equivalent to the length of the repeat unit (1.33 nm) of the cyclic polymer. The energy may be rewritten in discrete form in terms of $\{s_i\}$, where $s_i = r_i - r_{i-1}$ (see inset of Figure 4A). A further constraint is that the bending angle at

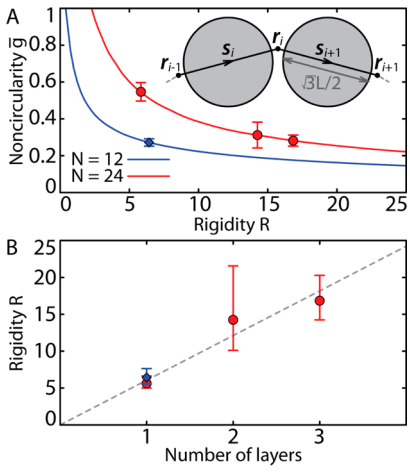

Figure 4. (A) Plot of simulation results of $\bar{g}$ against R for $N = 12$ and $N = 24$ with experimental data points placed on the curves. Inset: Schematic diagram showing a section of the nanoring model. (B) Extracted R values plotted against the number of layers in a nanoring, with a linear line of best fit with zero intercept and slope of 6.06.

dx.doi.org/10.1021/nl4017557 | Nano Lett. 2013, 13, 3391–3395

each linking point is limited to 60° by placing hard discs (overlapping of which costs an infinite energy penalty) with radii $\sqrt{3}L/2$ at the midpoints between bending points. To generate thermally equilibrated nanorings obeying these energetics, Monte Carlo simulations are performed using the Metropolis algorithm (see Supporting Information for more details). The characteristic bending, κ_B/L, and thermal, kT, energies are the only relevant energy scales and the calculated behavior is determined only by the ratio $R = \kappa_B/LkT$ which may be considered as a dimensionless rigidity.

Figure 4A shows the variation of $\overline{g}$ with R for $N = 12$ and $N = 24$ with the experimental points overlaid. As expected, the departure from circularity increases if the stiffness decreases or the number of bending points increases. From these results the value of R can be estimated from the measured values of $\overline{g}$, and the inferred dependence of R on the stack height is shown in Figure 4B. Of particular significance is the near equality, within experimental error, of R for single layers of c-P12 and c-P24. This is expected since κ_B and L, which determine R, depend only on the chemical nature of the polymer repeat unit and are independent of nanoring size. This equality provides strong support for our theoretical approach based on rings in thermal equilibrium. Furthermore Figure 4B shows a linear dependence of R on stack height with zero intercept and a slope of 6 ± 1. This result indicates that the bending stiffness κ_B has a simple linear dependence on the stack height.

Using a value of $kT \approx 25$ meV corresponding to room temperature, the bending rigidity of single layered nanorings is $\kappa_B \approx 0.03$ nN·nm^2 (rising to 0.07 nN·nm^2 and 0.10 nN·nm^2 for double and triple layers, respectively). Furthermore we can estimate the persistence length for an analogue single-layer linear polymer, $l_P = \kappa_B/kT \sim 8$ nm.[32] This value is significantly lower than the correlation length ~25 nm measured previously for linear porphyrin polymers. This difference arises from the parallel alignment of neighboring densely packed linear polymers, as discussed in our previous work,[5] which is not relevant for the isolated nanorings which we consider here.

Our results imply that the bending stiffness of the nanoring stacks is approximately equal to the sum of the contributions of the component rings. This suggests that the interactions which stabilize the stacking are only weakly affected by bending. This observation is consistent with a model whereby the interactions between nanorings in a stack are dominated by the coplanar stacking of porphyrin macrocycles, which is assumed here to arise from $\pi-\pi$ interactions, whereas the in-plane bending is dominated by the butadiyne linker groups. These latter groups would be expected to have a weaker and less directional interaction with equivalent groups in adjacent stack layers. While we believe this model is plausible, it implies a specific relative positioning of porphyrins in adjacent layers. The registry of buried layers cannot be determined from our STM images with confidence although our images are consistent with rings stacking directly on top of each other without any obvious offset, and the positions of the 24 porphyrin groups in the top layer of the stack can be resolved in many images (see Supporting Information for an example). In contrast the partially overlapping rings discussed earlier (and identified in Figure 2) cross at angles close to 90° consistent with our previous studies of overlapping linear analogue polymers.

The histogram in Figure 3 implies that a stack of three nanorings (height 0.7 nm) is particularly stable. For a simple aggregation of nanorings we would expect a monotonic decrease in the frequency of occurrence for stacks with increasing layer numbers. However in the absence of THF we find that the three-layer stacks are much more frequently observed than the two layer stacks, while for added THF the frequencies are approximately equal. In addition we observe no four stacks in the absence of THF and a very small fraction when THF is added. This implies that the three layer stack has enhanced stability. Although the mechanism for this enhancement is unclear at this stage, it may be associated with steric effects arising from the packing of the solubilizing side groups.

Our results show that supramolecular organization of synthetic molecular nanostructures can result in a modification of collective properties of the resulting aggregate giving rise, in this example to an enhanced mechanical stiffness. In addition we have shown that the effect is controlled by choice of solvent and is preserved following transfer by electrospray from solution onto a clean surface held under vacuum. The largest aggregate observed has a molecular weight >100 kDa, comparable with large protein molecules. Previous work on linear porphyrin-based molecular wires has demonstrated that the formation of supramolecular stacks can facilitate charge transport by enhancing electronic coupling and creating a narrower distribution of electronic states along the chain.[36,37] The nanorings discussed here are of great interest since their large size and extended π conjugation holds promise for the exploration of Aharonov–Bohm effects at the molecular level.[38,39] The columnar stacking we observe will be important for such studies since they suppress randomness in shape and stabilize a near-circular conformation with maximal enclosed large areas as required for currently accessible high magnetic fields.

■ ASSOCIATED CONTENT

Supporting Information

Experimental protocols, additional results, and further information related to the computer simulations. This material is available free of charge via the Internet at http://pubs.acs.org.

■ AUTHOR INFORMATION

Corresponding Author

*E-mail: peter.beton@nottingham.ac.uk.

Notes

The authors declare no competing financial interest.

■ ACKNOWLEDGMENTS

We thank the U.K. Engineering and Physics Sciences Research Council for financial support through grants EP/J006939/1 and EP/J007161/1. A.S. thanks the University of Nottingham for the award of Nottingham Advanced Research Fellowship. D.V.K. thanks the Clarendon Fund (University of Oxford) for support.

■ REFERENCES

(1) Bartels, L. *Nat. Chem.* **2010**, *2*, 87–95.
(2) Barth, J. V.; Costantini, G.; Kern, K. *Nature* **2005**, *437*, 671–9.
(3) Kudernac, T.; Lei, S.; Elemans, J. A. A. W.; De Feyter, S. *Chem. Soc. Rev.* **2009**, *38*, 402–21.
(4) Lafferentz, L.; Ample, F.; Yu, H.; Hecht, S.; Joachim, C.; Grill, L. *Science* **2009**, *323*, 1193–7.
(5) Saywell, A.; Sprafke, J. K.; Esdaile, L. J.; Britton, A. J.; Rienzo, A.; Anderson, H. L.; O'Shea, J. N.; Beton, P. H. *Angew. Chem., Int. Ed.* **2010**, *49*, 9136–9.

(6) Mena-Osteritz, E.; Meyer, A.; Langeveld-Voss, B. M. W.; Janssen, R. A. J.; Meijer, E. W.; Bäuerle, P. *Angew. Chem., Int. Ed.* **2000**, 2679−2684.
(7) Scifo, L.; Dubois, M.; Brun, M. E. L.; Rannou, P.; Latil, S.; Rubio, A.; Grévin, B. *Nano Lett.* **2006**, *6*, 1711−8.
(8) Deng, Z.; Thontasen, N.; Malinowski, N.; Rinke, G.; Harnau, L.; Rauschenbach, S.; Kern, K. *Nano Lett.* **2012**, *12*, 2452−8.
(9) Lingenfelder, M.; Tomba, G.; Costantini, G.; Colombi Ciacchi, L.; De Vita, A.; Kern, K. *Angew. Chem., Int. Ed.* **2007**, *46*, 4492−5.
(10) Klappenberger, F.; Cañas-Ventura, M. E.; Clair, S.; Pons, S.; Schlickum, U.; Qu, Z.-R.; Brune, H.; Kern, K.; Strunskus, T.; Wöll, C.; Comisso, A.; De Vita, A.; Ruben, M.; Barth, J. V. *ChemPhysChem* **2007**, *8*, 1782−6.
(11) Mössinger, D.; Chaudhuri, D.; Kudernac, T.; Lei, S.; De Feyter, S.; Lupton, J. M.; Höger, S. *J. Am. Chem. Soc.* **2010**, *132*, 1410−23.
(12) Anderson, H. L. *Chem. Commun.* **1999**, 2323−2330.
(13) Bonnett, R. *Chem. Soc. Rev.* **1995**, *24*, 19−33.
(14) O'Sullivan, M. C.; Sprafke, J. K.; Kondratuk, D. V.; Rinfray, C.; Claridge, T. D. W.; Saywell, A.; Blunt, M. O.; O'Shea, J. N.; Beton, P. H.; Malfois, M.; Anderson, H. L. *Nature* **2011**, *469*, 72−5.
(15) Kondratuk, D. V.; Perdigao, L. M. A.; O'Sullivan, M. C.; Svatek, S.; Smith, G.; O'Shea, J. N.; Beton, P. H.; Anderson, H. L. *Angew. Chem., Int. Ed.* **2012**, *51*, 6696−9.
(16) Iyoda, M.; Yamakawa, J.; Rahman, M. J. *Angew. Chem., Int. Ed.* **2011**, *50*, 10522−53.
(17) Sprafke, J. K.; Kondratuk, D. V.; Wykes, M.; Thompson, A. L.; Hoffmann, M.; Drevinskas, R.; Chen, W.; Yong, C. K.; Kärnbratt, J.; Bullock, J. E.; Malfois, M.; Wasielewski, M. R.; Albinsson, B.; Herz, L. M.; Zigmantas, D.; Beljonne, D.; Anderson, H. L. *J. Am. Chem. Soc.* **2011**, *133*, 17262−73.
(18) Fenwick, O.; Sprafke, J. K.; Binas, J.; Kondratuk, D. V.; Di Stasio, F.; Anderson, H. L.; Cacialli, F. *Nano Lett.* **2011**, *11*, 2451−6.
(19) McDermott, G.; Prince, S. M.; Freer, A. A.; Hawthornthwaite-Lawless, A. M.; Papiz, M. Z.; Cogdell, R. J.; Isaacs, N. W. *Nature* **1995**, *374*, 517−521.
(20) Scheuring, S.; Seguin, J.; Marco, S.; Lévy, D.; Robert, B.; Rigaud, J.-L. *Proc. Natl. Acad. Sci.* **2003**, *100*, 1690−3.
(21) Rauschenbach, S.; Stadler, F. L.; Lunedei, E.; Malinowski, N.; Koltsov, S.; Costantini, G.; Kern, K. *Small* **2006**, *2*, 540−7.
(22) Saywell, A.; Magnano, G.; Satterley, C. J.; Perdigão, L. M. A.; Champness, N. R.; Beton, P. H.; O'Shea, J. N. *J. Phys. Chem. C* **2008**, *112*, 7706−7709.
(23) Saywell, A.; Magnano, G.; Satterley, C. J.; Perdigão, L. M. A.; Britton, A. J.; Taleb, N.; Del Carmen Giménez-López, M.; Champness, N. R.; O'Shea, J. N.; Beton, P. H. *Nat. Commun.* **2010**, *1*, 75.
(24) Auwärter, W.; Seufert, K.; Bischoff, F.; Ecija, D.; Vijayaraghavan, S.; Joshi, S.; Klappenberger, F.; Samudrala, N.; Barth, J. V. *Nat. Nanotechnol.* **2012**, *7*, 41−6.
(25) Tanaka, H.; Kawai, T. *Nat. Nanotechnol.* **2009**, *4*, 518−22.
(26) Grill, L.; Dyer, M.; Lafferentz, L.; Persson, M.; Peters, M. V.; Hecht, S. *Nat. Nanotechnol.* **2007**, *2*, 687−91.
(27) Yokoyama, T.; Yokoyama, S.; Kamikado, T.; Okuno, Y.; Mashiko, S. *Nature* **2001**, *413*, 619−21.
(28) Spillmann, H.; Kiebele, A.; Stöhr, M.; Jung, T. A.; Bonifazi, D.; Cheng, F.; Diederich, F. *Adv. Mater.* **2006**, *18*, 275−279.
(29) Blunt, M. O.; Russell, J. C.; Gimenez-Lopez, M. D. C.; Taleb, N.; Lin, X.; Schröder, M.; Champness, N. R.; Beton, P. H. *Nat. Chem.* **2011**, *3*, 74−8.
(30) Hunter, C. A.; Sanders, J. K. M. *J. Am. Chem. Soc.* **1990**, *112*, 5525−5534.
(31) Screen, T. E. O.; Blake, I. M.; Rees, L. H.; Clegg, W.; Borwick, S. J.; Anderson, H. L. *J. Chem. Soc., Perkin Trans. 1* **2002**, 320−329.
(32) Anderson, H. L. *Inorg. Chem.* **1994**, *33*, 972−981.
(33) Screen, T. E. O.; Thorne, J. R. G.; Denning, R. G.; Bucknall, D. G.; Anderson, H. L. *J. Mater. Chem.* **2003**, *13*, 2796.
(34) Ziherl, P. *Phys. Rev. Lett.* **2007**, *99*, 128102.
(35) Seifert, U. *Phys. Rev. A* **1991**, *43*, 6803−6814.
(36) Kocherzhenko, A. A.; Patwardhan, S.; Grozema, F. C.; Anderson, H. L.; Siebbeles, L. D. A. *J. Am. Chem. Soc.* **2009**, *131*, 5522−9.
(37) Grozema, F. C.; Houarner-Rassin, C.; Prins, P.; Siebbeles, L. D. A.; Anderson, H. L. *J. Am. Chem. Soc.* **2007**, *129*, 13370−1.
(38) Mayor, M.; Didschies, C. *Angew. Chem., Int. Ed.* **2003**, *42*, 3176−9.
(39) Kleemans, N.; Bominaar-Silkens, I.; Fomin, V.; Gladilin, V.; Granados, D.; Taboada, A.; García, J.; Offermans, P.; Zeitler, U.; Christianen, P.; Maan, J.; Devreese, J.; Koenraad, P. *Phys. Rev. Lett.* **2007**, *99*, 146808.